



Severe growth disturbances in an early Permian calamitalean – traces of a lightning strike?

by

LUDWIG LUTHARDT, MATHIAS MERBITZ, and RONNY RÖBLER

With 10 text-figures and 1 table

Abstract

Woody trees are regarded as excellent natural data archives, even far back in geological time. In addition to regular growth patterns, destruction scars bear witness to various kinds of growth disturbances which are recorded as a result of environmental impact during the life time of a tree. Although stem injuries can provide significant insight into plant-environment interactions, only minor attention has been paid to this subject in the fossil record. Here, we present a fossil scar documented in a petrified, basal calamitalean stem (*Arthropitys bistriata*) found in growth position in the early Permian Chemnitz Fossil Forest (SE-Germany). Because this forest was buried under volcanic deposits in a geological instant (i.e., a T⁰ assemblage), the fossil lagerstätte permits detailed investigations of anatomically preserved plants and their environment. The special injury of the calamitalean described herein extends to 40 % of the stem circumference, exhibits an elongated to triangular shape, a central furrow, a scar-associated event ring of collapsed to distorted tracheids, and was ultimately overgrown by callus parenchyma. We suggest that this scar most likely was caused by a lightning strike, as two first order roots, still attached to the stem, show injuries, whereas the neighbouring trees at the excavation site seem to be unaffected. In response to this severe injury, the tree completely recovered within a relatively short time of ca. 12 years, revealing stress-induced rapid growth rates indicated by wide tree rings and large, thin-walled tracheids, and probable basal sprouting. Several scars of various shapes have been recognised in other specimens in the Chemnitz collection and excavation material suggesting multifaceted plant-environment interactions within this early Permian forest ecosystem.

Keywords: Chemnitz Fossil Forest; T⁰ assemblage; wood anatomy; tree damage; dendroecology

Contents

1 Introduction	2	4.5.1 The palaeosol – former substrate of the <i>in situ</i> tree	14
2 Geological setting	2	4.5.2 Crown remains	15
3 Material and methods	5	4.5.3 Neighbouring trees of KH0277	15
4 Results	6	5 Discussion	15
4.1 Anatomy of KH0277	6	5.1 Reconstruction of KH0277	15
4.2 Stem damage	6	5.2 Potential causes of damage	16
4.3 Root damage	13	5.3 Plant recovery response	19
4.4 Tree-ring record	13	6 Conclusions	19
4.5 Periphery of KH0277	13	Acknowledgements	20
		References	20

Authors' addresses:

LUDWIG LUTHARDT, MATHIAS MERBITZ, RONNY RÖBLER, Museum für Naturkunde Chemnitz, Moritzstraße 20,
09111 Chemnitz, Germany.

luthardt@mailserver.tu-freiberg.de (corresponding author)

LUDWIG LUTHARDT, RONNY RÖBLER, Geological Institute, Technische Universität Bergakademie Freiberg,
Bernhard-von-Cotta-Straße 2, 09599 Freiberg, Germany

1 Introduction

The Chemnitz Fossil Forest represents a diverse fossil assemblage, which allows detailed studies of ecological processes and relationships in an early Permian forest ecosystem, both in space and time (RÖBLER et al. 2012a). Investigation of biotic elements and understanding of their role in a web of intricate environmental interactions is the major focus of investigations in this palaeo-ecosystem. To date, diverse studies on various groups of organisms reflect the great potential of this unique fossil lagerstätte (RÖBLER 2000; RÖBLER & NOLL 2006; RÖBLER & NOLL 2010; RÖBLER et al. 2008; RÖBLER et al. 2009; RÖBLER et al. 2010; RÖBLER et al. 2012a; RÖBLER et al. 2012b; RÖBLER et al. 2014; FENG et al. 2012; FENG et al. 2014; DUNLOP & RÖBLER 2013; DUNLOP et al. 2016; LUTHARDT et al. 2016; SPINDLER et al. 2018).

The capability to assess palaeoecological and palaeoenvironmental processes even in their fourth dimension by dendrochronological and -ecological methods has been recently demonstrated (LUTHARDT & RÖBLER 2017a; LUTHARDT & RÖBLER 2017b; LUTHARDT et al. 2017). As a result, tree rings were interpreted to depict a high-resolution climate archive revealing climatic oscillations most likely caused by the 11-year solar cycle (LUTHARDT & RÖBLER 2017a). Different types of tree rings were recorded by pycnoxylic gymnosperms, calamitaleans and medullosan seed ferns, and differentiated, based on their morphological features (LUTHARDT et al. 2017). Among these tree-ring types, so called event rings (Type 3 according to LUTHARDT et al. 2017) appear among the most conspicuous growth interruptions. They occur in transverse sections of all investigated plants as solitary zones of injured living wood and are overgrown by parenchymatous callus tissue (LUTHARDT et al. 2017). Subtypes 3b and 3c only occur in calamitaleans and medullosans, and are interpreted to record episodes of exceptionally severe drought.

Subtype 3a, however, involves distinct scars, resulting from stem injuries caused by catastrophic environmental events. As there are several potential interpretations, deciphering scar formation processes in fossil trees remains challenging. This may be one reason that only minor attention has been paid to this field of research in the fossil record, although it may offer considerable potential for palaeoenvironmental reconstructions. Some recent studies focus on comparable phenomena in fossil trees and reflect a rising interest in this field (e.g., BYERS et al. 2014;

FALCON-LANG et al. 2015; FENG et al. 2017). Additionally, fossil stem injuries may provide inferences on wound-healing strategies of extinct plants, and the vitality of tree populations in ancient forest ecosystems in general.

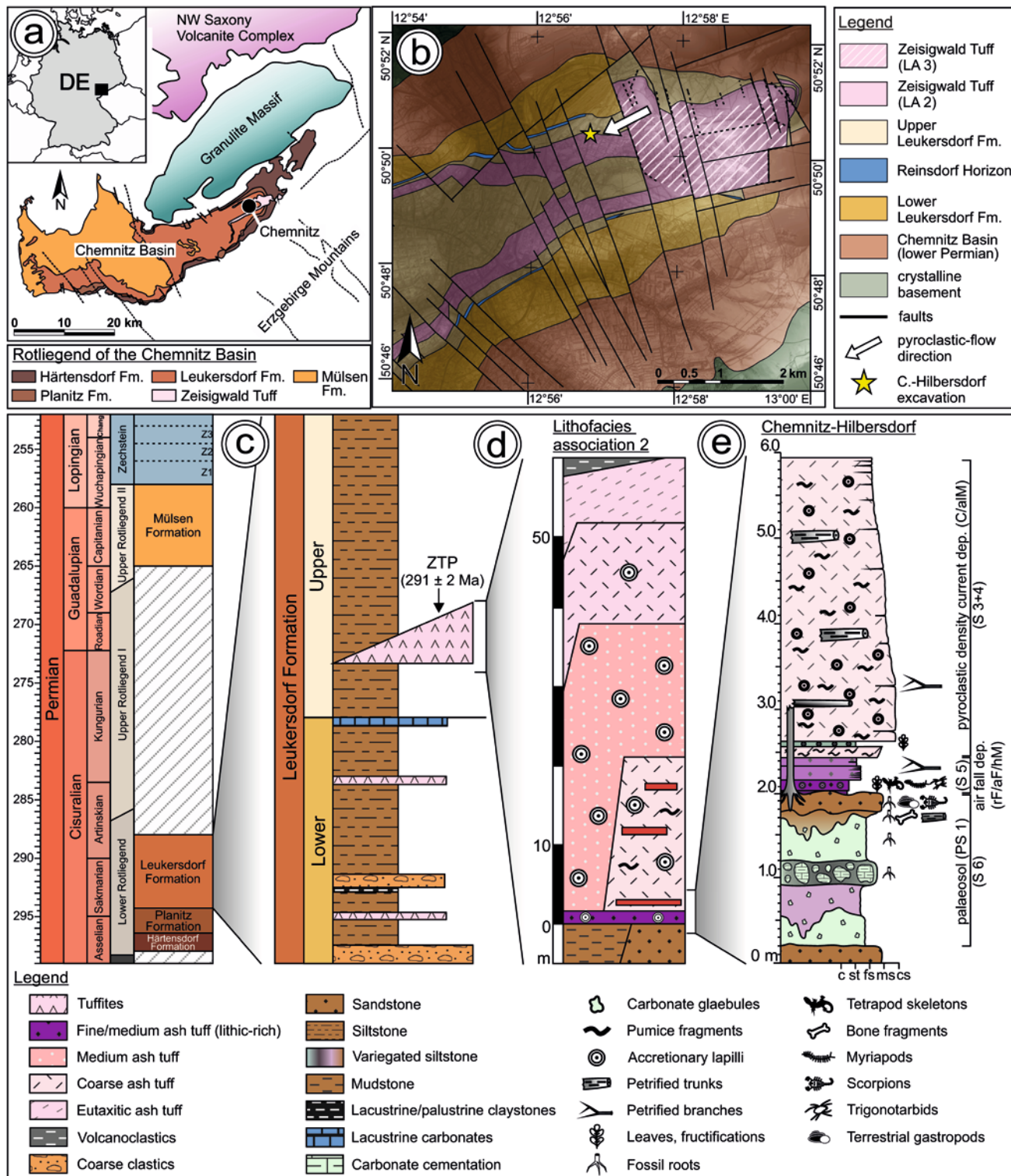
Trees in the Chemnitz Fossil Forest were buried simultaneously in their places of growth by a series of pyroclastic deposits during a volcanic event. Therefore, they represent a true T⁰ assemblage (GASTALDO et al. 1995; DIMICHELE & FALCON-LANG 2011). The tree-ring record obtained from the forest community encompasses nearly 80 years, whereas single scars were found in the stem sections at several instances within this time span (LUTHARDT et al. 2017). Among them is a prominent stem injury in specimen KH0277, a tall calamitalean tree identified as *Arthropitys bistrata* (COTTA 1832) RÖBLER et al. 2012 and found in an upright position at the Chemnitz-Hilbersdorf excavation (RÖBLER et al. 2012a; RÖBLER et al. 2014; LUTHARDT et al. 2016; LUTHARDT et al. 2017).

The first note about a scar in a petrified trunk from the Chemnitz Fossil Forest was provided by GOEPPERT (1881). Referring to an *Agathoxylon* sp. trunk of 2.24 m extent, he described an elongated, fissure-shaped scar, which shows a bulbous to elongated overgrowth of wounded wood, reminding him of frost cracks (GOEPPERT 1881: plate III, fig. 8).

The scope of this contribution is to evaluate potential causes of a major injury and resulting recovery reactions in the calamitalean KH0277 by applying palaeobotanical and dendroecological methods to a volcanoclastic T⁰ assemblage. Results shed light on unusual plant-environment interactions within a short time span of several decades in an early Permian forest ecosystem.

2 Geological setting

The study site is located in the Chemnitz Basin (Saxony, SE-Germany), which is part of the eastern Saxothuringian zone and is bordered by Variscan metamorphic units of the Erzgebirge to the South and the Granulite Massif to the North (Text-fig. 1a). With an extent of 70 × 30 km, it represents one of the small intramontane Rotliegend basins in Central Europe (SCHNEIDER et al. 2010). The Chemnitz Basin developed during the post-orogenic phase of the Variscids and is composed of a 1,550 m thick succession of predominantly continental red bed sedimentary rocks of early to late Permian age (Asselian–Wuchiapingian, Text-fig. 1c). Based on six sedimentary megacycles, the



Text-fig. 1. Geological setting of the Chemnitz Fossil Lagerstätte: **a** – Geographical and geological overview. **b** – Detailed geological map of the study area in Chemnitz showing the distribution of the entombing Zeisigwald Tuff pyroclastics and the position of the Chemnitz-Hilbersdorf excavation. **c** – Stratigraphy of the Leukersdorf Formation (Chemnitz Basin) and position of the Zeisigwald Tuff pyroclastics. **d** – Lithological profile of the widely distributed lithofacies association 2 (LUTHARDT et al. 2018) of the Zeisigwald Tuff pyroclastics. **e** – Chemnitz-Hilbersdorf excavation profile showing the basal pyroclastics.

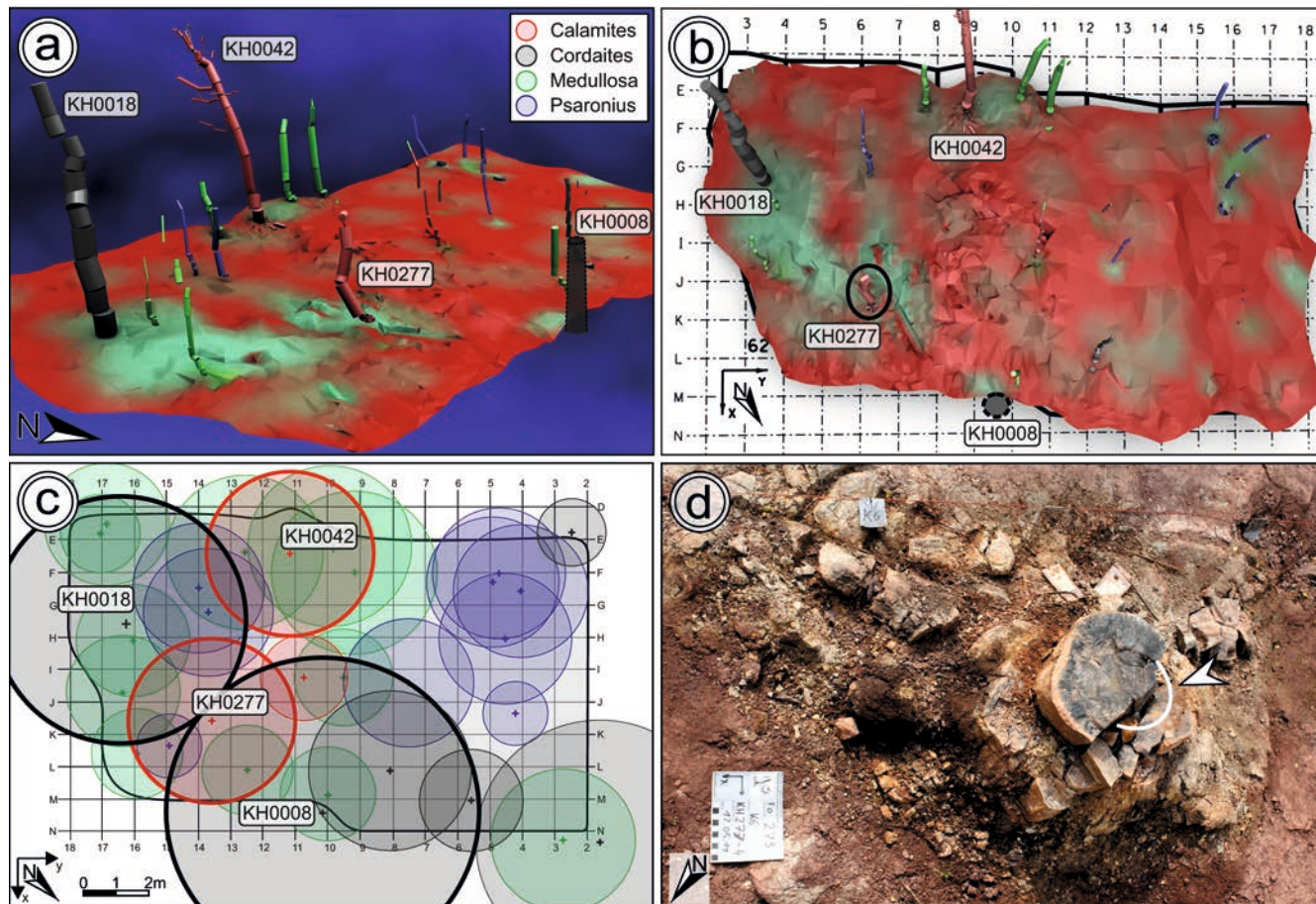
strata are subdivided into four formations (SCHNEIDER et al. 2012).

The fossil forest is located in the north-eastern branch of the Chemnitz Basin, in the city of Chemnitz, and is part of the Upper Leukersdorf Formation (Text-fig. 1b, c). Alluvial wet red beds (*sensu* SCHNEIDER et al. 2010) dominate the 800 m thick succession of the entire Leukersdorf Formation, which can be subdivided into three sedimentary mesocycles. The sequence is characterised by several marker horizons, such as the lacustrine-palustrine Rottluff Coal Horizon, the lacustrine Reinsdorf Carbonate Horizon and several intercalated pyroclastics (SCHNEIDER et al. 2012). In the Upper Leukersdorf Formation, the most prominent pyroclastic horizon is the Zeisigwald Tuff that hosts the Chemnitz Fossil Lagerstätte and provides an isotopic age of 291 ± 2 Ma (LUTHARDT et al. 2018). Originating from a small and highly specialised magma, the Zeisigwald Tuff pyroclastics were deposited during a plinian eruption with a phreatomagmatic character, resulting in an up to 90 m thick succession of rhyolitic ash tuffs, which extend over nearly the whole area of the city of Chemnitz (Text-fig. 1b) (FISCHER 1990; EULENBERGER et al. 1995). The volcanic event is assumed to have been a continuous process of multiple eruptions, whereas eruption energy gradually increased (LUTHARDT et al. 2018). Early stages of the eruption resulted in minor fallout deposits from an ash column, preserving floral and faunal elements *in situ* as adpressions within a ca. 0.50 m thick succession of fine- to medium-grained ash tuff. Thereafter, diluted to concentrated pyroclastic flows buried extended parts of a multi-aged diverse forest ecosystem. Pyroclastic flows broke and/or toppled trees, which generally exhibit an ENE-WSW orientation (Text-fig. 1b). The final major eruption phase resulted in deposition of widely distributed and massive ignimbrite deposits (LUTHARDT et al. 2018).

Investigated material is derived from the scientific excavation in Chemnitz-Hilbersdorf (2008–2011), where, among many other fossils, 53 stems were found in growth position over an area of 24 by 18 m. The excavation profile shows three major lithological units, encompassing a clastic palaeosol horizon (Unit S6), which is overlain by the basal pyroclastic deposits of Units S5/4 and S3 (Text-fig. 1d, e). The palaeosol horizon measures ca. 2 m in thickness, and developed on red-coloured fine clastics of a seasonally wet alluvial floodplain. At the top, the palaeosol comprises a red-coloured, sandy substrate that shows a surprisingly low degree of chemical weathering (LUTHARDT

et al. 2016). Down to a depth of 0.40 m, the palaeosol is densely pervaded by roots of various sizes, usually preserved as sediment casts with marginal bleached haloes filled with manganese and iron oxides. The lower section of the palaeosol is light green coloured with, in places, violet mottling, as well as massive carbonate formation, which is interpreted as a groundwater calcrete (LUTHARDT et al. 2016). The palaeosol was formed under a strongly seasonal palaeoclimate and sub-humid conditions with precipitation rates of 800–1,100 mm/a (LUTHARDT et al. 2016). The 0.54–0.61 m thick pyroclastic Units S5 and S4 overlie Unit S6 with a sharp contact, and are a series of purple to light grey coloured, horizontally bedded ash tuffs, which generally bear many lithic fragments as well as accretionary lapilli at the base (S5.1) and top (S4). The succession is interpreted as a series of fallout deposits with a horizontal transport component (S5.1–5.3) and a minor flow deposit (S5.4) with an associated ash cloud layer (S4). Sub-unit S5.1 is the major fossil bearing horizon with numerous plant adpressions and various animal remains (RÖBLER et al. 2009; RÖBLER et al. 2012b; DUNLOP & RÖBLER 2013; FENG et al. 2014; DUNLOP et al. 2016; SPINDLER et al. 2018). Unit S3 overlies Unit S4 with an erosive contact and represents a > 3.35 m thick, light-red to purple-red coloured, unwelded lapilli tuff horizon, although the original thickness is not preserved due to surface weathering. Unit S3 is rich in lithics, pumice fragments and accretionary lapilli. As it hosts transported and horizontally embedded stems and branches, this unit is interpreted as a concentrated pyroclastic flow deposit.

During the continuous eruption process, plants and animals were killed almost simultaneously. In combination with the autochthonous to sub-autochthonous burial, this fossil lagerstätte is interpreted as a true T⁰ assemblage. At the excavation site Chemnitz-Hilbersdorf, the 53 plants in upright position once represented a hygrophilous vegetation community composed of medullosan seed ferns (*M. stellata* var. *typica* and *M. stellata* var. *lignosa*, 35%), cordaitaleans (*Cordaixylon* sp., 30%), tree ferns of the distichous type (*Psaronius* sp., 22%) and calamitaleans (*Arthropitys bistriata*, *Arthropitys ezonata*, ?*Arthropitys sterzelii*, 13%), whereas 30% of the 53 stems remain unidentified due to inadequate preservation. Many of the stems were broken off at a height of ca. 1.5 m by the destructive force of the pyroclastic flow of Unit S3, and carried several metres away.



Text-fig. 2. Position of the calamitalean KH0277 in the Chemnitz-Hilbersdorf excavation: **a** – 3D model of the excavated area showing KH0277 and large neighbouring trees. **b** – Top view on the excavated area. **c** – Top view on excavation raster showing position of *in situ* upright plants and their approximated crown diameter. **d** – Basal stem of KH0277 with root system after removal of the uppermost palaeosol horizon; white line and arrow indicate the position of the scar.

3 Material and methods

The petrified stem of the basal calamitalean KH0277 was excavated between 2009 and 2011 in the Chemnitz-Hilbersdorf excavation (N 50° 51' 9.85", E 12° 56' 45.95"). It was found in growth position, anchored in the palaeosol and entombed by overlying pyroclastic deposits (located in excavation grid: J-K/6-7, FP0175). Position and orientation of the stem were measured at several points by a tachymeter to integrate data in a 3D model that enables visualisation of the spatial distribution of finds (Text-fig. 2a, b). Most likely due to the destructive force of the pyroclastic density current (Unit S3), the KH0277 tree was broken at a height of ca. 1.65 m, whereas the uppermost part of the stem must have been embedded horizontally within Unit S3. Because a clear indication for linkage to several horizontally orientated stems in the excavation area cannot be provided, e.g. to KH0052 (*A. bistriata*; FENG et al. 2012; RÖBLER et al. 2012b), the original architecture of the whole plant cannot be reconstructed in detail.

Resulting from sub-recent slope movement of the embedding rocks, the specimen was broken into large segments and numerous small pieces. During excavation, four stem sections were differentiated: KH0277-01/-02/-03/-04. Cutting of the stem provided six transverse sections (A–E, G in Text-fig. 3a), which were polished to gain three-dimensional information on scar morphology and anatomy. Transverse sections F and H represent fractured surfaces and were only used for macroscopic documentation. The other transverse sections were scanned by an Epson Perfection V330 Photo scanner, producing high-resolution images. Additionally, transverse sections of the silicified first order roots KH0546, KH0545 and KH0554 found *in situ* in the palaeosol (Unit S6) were examined for any indications of damage. Documentation and microphotography were performed under a Nikon SMZ 1500 microscope, equipped with a Nikon DS-5 M-L1 camera. Measurements of cell and tree-ring parameters were processed manually by microscopic camera software (NIS Elements D 3.2). Raw ring width data were detrended and power-trans-

formed according to methods applied in LUTHARDT et al. (2017).

To assess the collateral impact of the destructive event that affected KH0277, large neighbouring trees at the excavation site, as well as several additional trees from Chemnitz-Hilbersdorf within a radius of ca. 750 m from the excavation (LUTHARDT et al. 2017), were examined for comparable damage patterns. Data on palaeosol sedimentological investigation provided by LUTHARDT et al. (2016) are used to falsify different scenarios of environmental impact. The anatomy of several deadwood specimens, which were found on the palaeosol surface or within the upper palaeosol horizon, was examined for their potential affinity to the KH0277 stem.

4 Results

4.1 Anatomy of KH0277

Cell preservation is generally moderate, although the quality is highly variable in the sections. In the uppermost part of KH0277-01, which is embedded in Unit S3, purple fluorite occurs as a petrification agent.

The stem exhibits extended secondary xylem surrounding the central pith, whereas the diameter decreases from 295×260 mm at the base (section G, KH0277-04) to 210×185 mm at the top (section A, KH0277-01). Based on the stem diameter of section A, positioned at breast height, the original stem height is reconstructed to ca. 17.6 m using the approximation given by MOSBRUGGER et al. (1994) and to 20.6 m applying the estimation of NIKLAS (1994), assuming a parenchyma portion of 45 % as documented for the species *A. bistriata* (RÖBLER et al. 2012a). It has been shown that the tree was rooting upon a cordaitalean deadwood trunk; the roots of different order are of *Astromylon* and *Asthenomyelon* types, and described as obliquely downward dipping first order roots (Text-fig. 4), which show departing second and third order roots arranged in node-like levels (RÖBLER et al. 2014).

The stem is symmetrically shaped and, therefore, once likely grew nearly vertically (Text-fig. 4). Altogether, three branching shoots showing secondary growth are evidenced, one in section G (KH0277-04, Text-fig. 3), another in section D (KH0277-02b) and the third in KH0277-01, the latter having collection number KH0276 (Text-fig. 3f). The shoot of section D has a diameter of 48 mm and shows at least three tree-rings (Text-fig. 3e). In the same section, an additional pith was recognised pointing to initial branching and origination of another woody side branch (Text-fig. 4).

The pith is incompletely preserved in most of the sections, due to compression and imperfect petrification. Compared to the stem diameter, the pith appears to be rather small at 7 mm in diameter (section G), but widens towards the top, reaching 35 mm in section B. Carinal canals are poorly preserved (Text-fig. 3b).

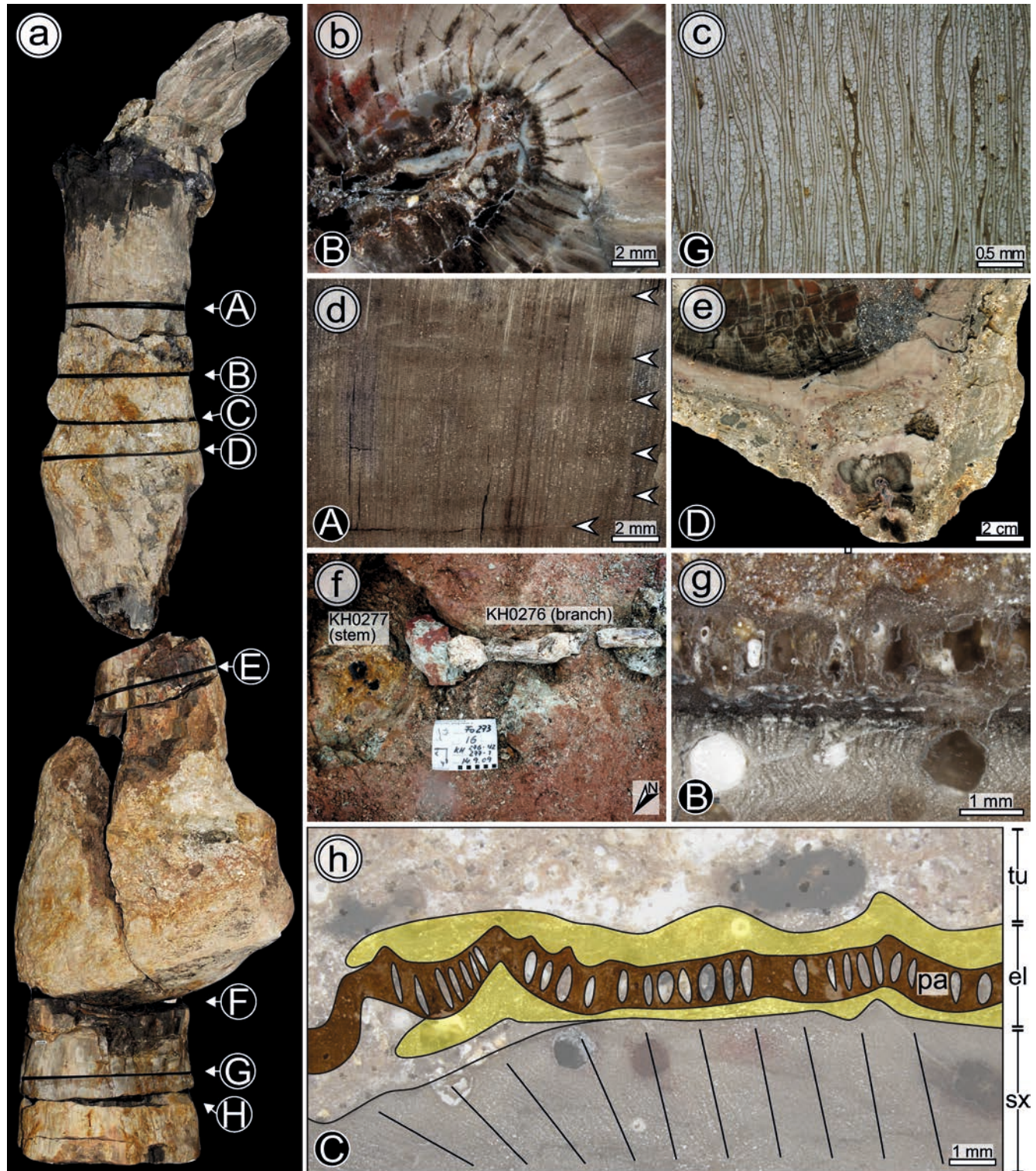
The secondary xylem is composed of radial tracheid files and parenchymatous rays, whereas usually 1–5 rows of tracheids occur between two interfascicular rays. Parenchymatous ray cells are thin-walled and sub-angular in shape whereas tracheids are more circular and thick-walled. In tangential section, the parenchyma portion was estimated at 45 % (Text-fig. 3c).

All transverse sections show circumferential tree rings, which are regular but indistinct (Text-fig. 3d), and hence referred to as Type 2 rings *sensu* LUTHARDT et al. (2017). Typically, these tree rings are narrow, compressed and show bent rows of tracheids in the outer wood, similar to descriptions provided by RÖBLER et al. (2012a). Additionally, event rings of Type 3a *sensu* LUTHARDT et al. (2017) occur in several transverse sections, which are described below.

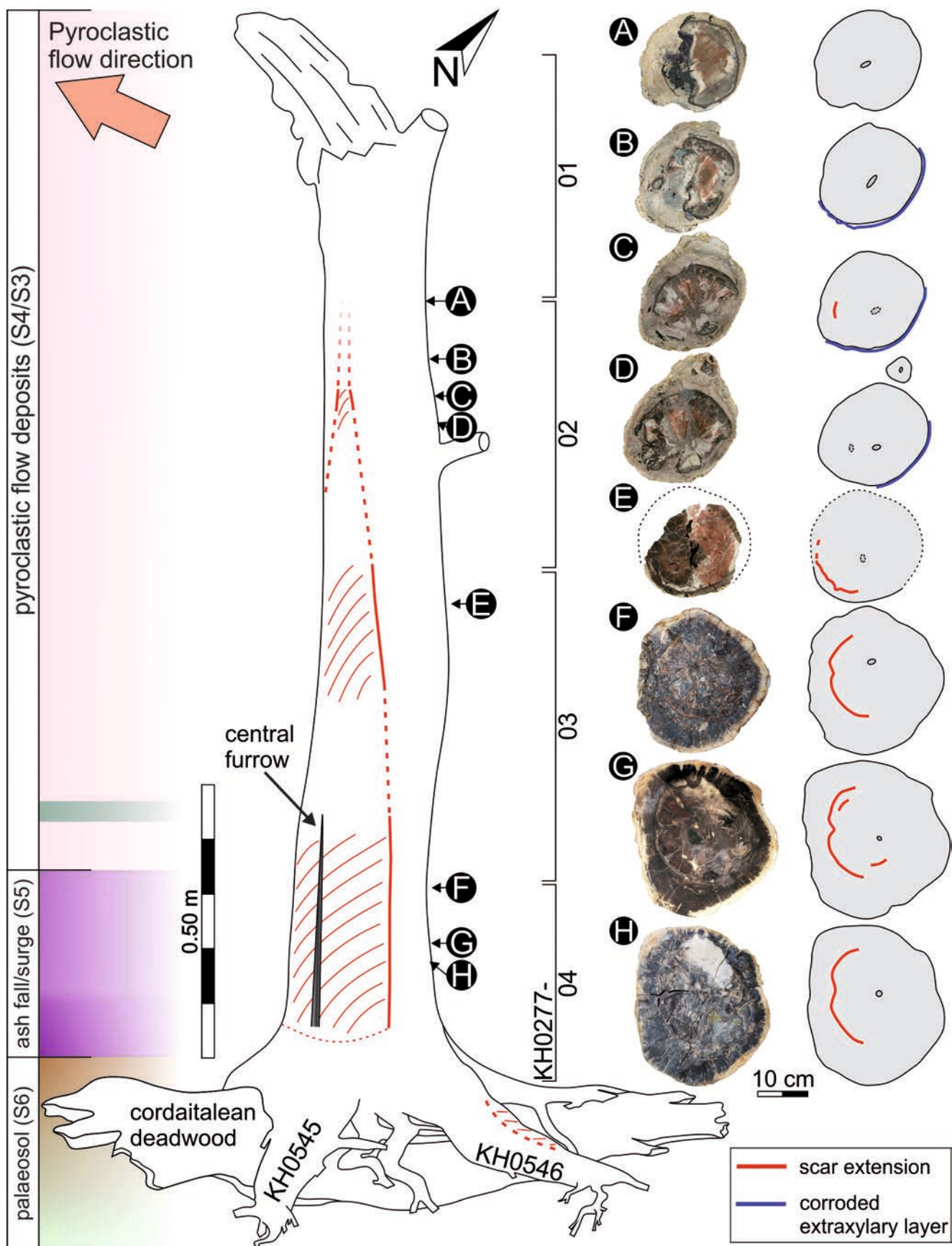
The broad secondary xylem is coated by a thin layer of extraxylary tissue differentiated by a characteristic cell structure. Bordering the secondary xylem with a sharp contact, this layer consists of one radial row of oval-shaped, palisade-like arranged voids mantled by undifferentiated tissue at the inner and outer margins (Text-fig. 3 g, h). The thickness of the layer varies between 2 and 25 mm. As the outer surface of the layer shows no relief in transverse sections, it is assumed that KH0277 was coated by a thin, smooth cortex. In several sections of the uppermost stem segment, this extraxylary layer is stripped off to one third of the stem circumference in an ENE direction (Text-figs. 3h, 7e), and thus facing the flow direction of the pyroclastic density current (from ENE to WSW). Hence, it is suggested that the extraxylary layer was partially abraded by pyroclastic material during the deposition of Unit S3.

4.2 Stem damage

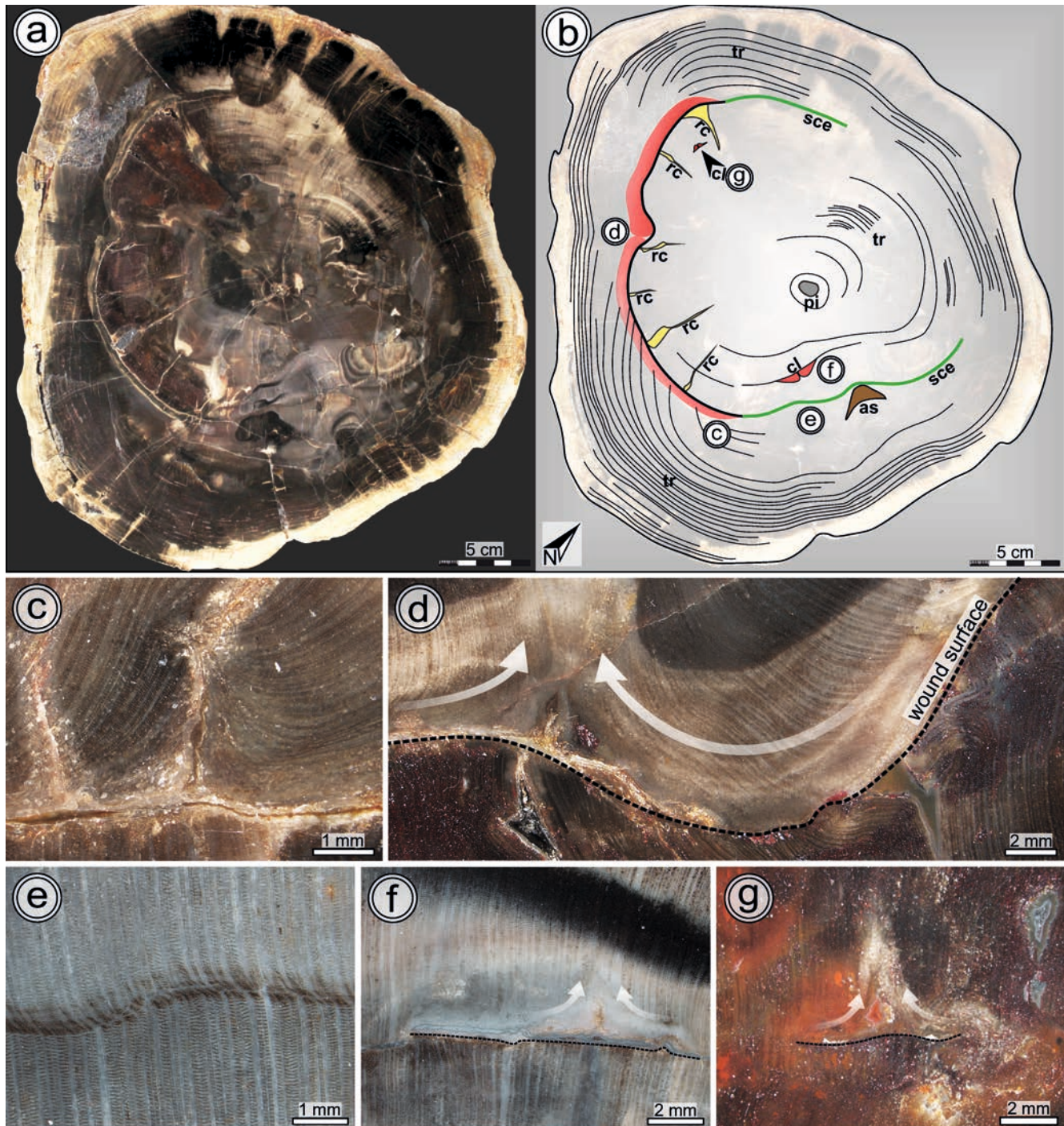
The injury zone, described as a Type 3a event ring *sensu* LUTHARDT et al. (2017), occurs in several transverse sections of KH0277 (Text-fig. 4), but was first recognised in section G of KH0277-04 (RÖBLER et al. 2014; LUTHARDT et al. 2016; LUTHARDT et al. 2017). The event ring is described as a non-circumferential band of destroyed to deformed tracheids, extending over 75 % of the whole stem circumference (Text-



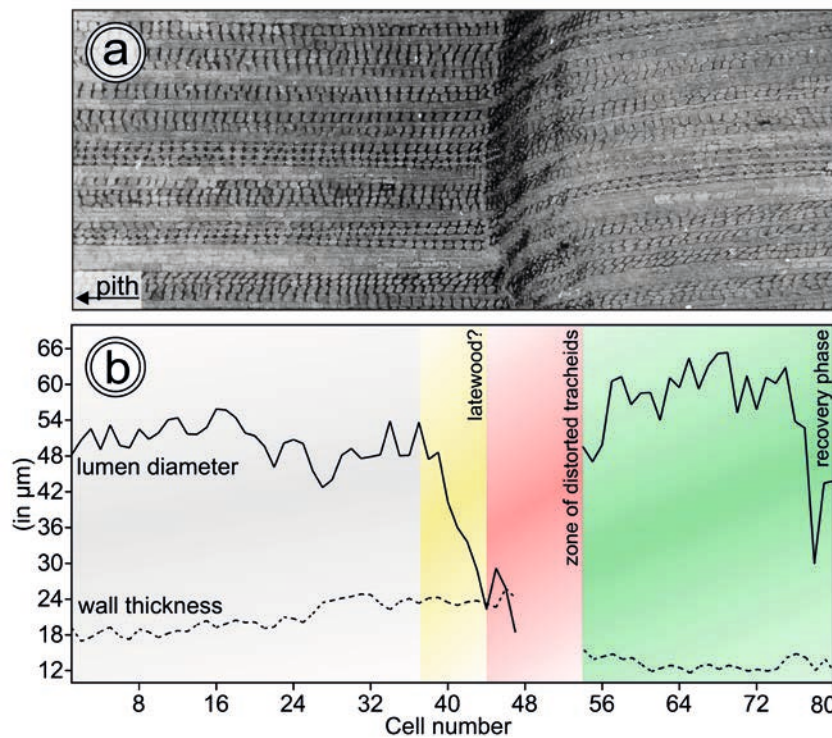
Text-fig. 3. Stem anatomy of the calamitalean KH0277 (*Arthropitys bistriata*). **a** – Basal stem with breakpoint at its top resulting from destruction by the pyroclastic density current and relicts of pyroclastic material still attached to the stem; position of sections A-H; length ca. 1.60 m. **b** – Central pith with carinal canals. **c** – Tracheids and ray parenchyma (45 %) in tangential section. **d** – Indistinct, but regular tree rings of Type 2 (LUTHARDT et al. 2017) in the outer wood. **e** – Side branch attached to the basal stem showing few tree rings. **f** – Calamitalean branch KH0276, most likely attached to the stem of KH0277 at the top. **g** – Detail of the extraxylary layer. **h** – Sketch from the photograph of the extraxylary layer (el) with palisade-like cells (pa) surrounding the wood (sx); on the left, extraxylary layer is removed by destructive force of the pyroclastic density current (tu).



Text-fig. 4. Reconstruction of the KH0277 basal stem including the root system (modified from RÖBLER et al. 2014). The stem shows the spatial distribution of the scar in the inner of the wood cylinder, reconstructed from sections A-H. On the left, major clastic and pyroclastic units from the excavation profile are illustrated to clarify taphonomical situation.



Text-fig. 5. Macroscopic and microscopic scar morphological characteristics in section G (KH0277-04). **a** – Scar morphology is indicated by colour variations in the polished section of KH0277-04. **b** – Sketch of major anatomical characteristics in section G (pi – pith, cl – callus tissue, sce – scar-associated band/event ring, rc – radial desiccation crack, as – adventitious shoot, tr – tree rings; numbers show position of the following images). **c** – Marginal initiation of callus tissue overgrowth, whereas tracheid rows suggest oriented growth from left to right. **d** – Central furrow overgrown by anastomosing callus tissue; secondary xylem shows minor distortion and radial cracks at the wound surface. **e** – Non-circumferential scar-associated event ring with a zone of distorted tracheids. **f** – Older, small scar of unknown origin in the inner wood. **g** – Another minor scar, probably of similar age as scar in “f”.



Text-fig. 6. Cell size variations in the scar-associated event ring of section G: **a** – Measured section showing the distinct zone of distorted and collapsed tracheids. **b** – Variations of lumen diameter and wall thickness throughout the section indicating latewood formation before the injuring event. Note distinctly larger and thin-walled cells after the event.

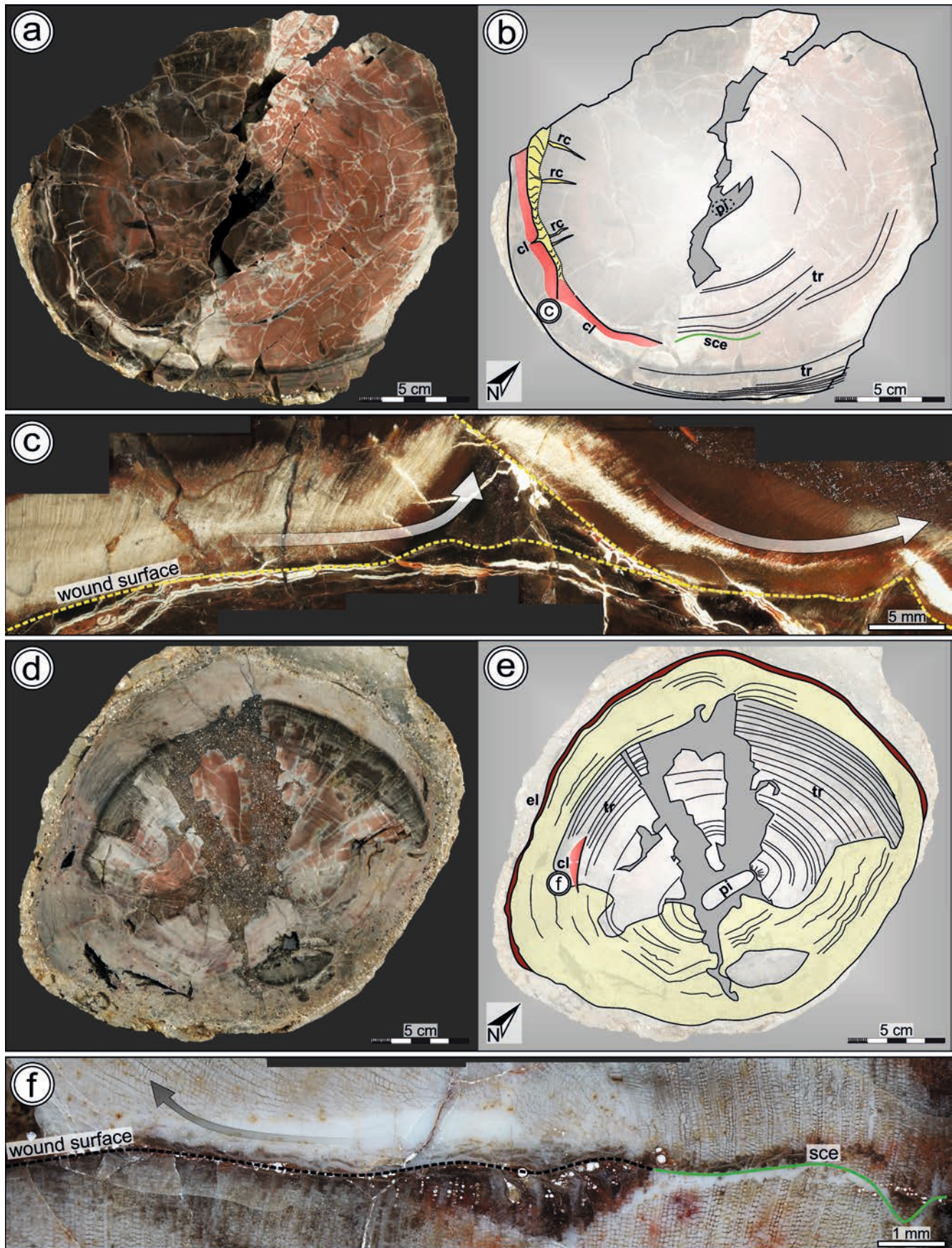
fig. 5a, b, e). Measurements of cell parameters in the event ring show slightly increasing tracheid wall thickness close to the event ring, whereas overall cell size remains stable (Text-fig. 6). The event ring itself is characterised by a rapid decrease of cell size with a sharp transition from normal tissue to a row of disrupted tracheids, followed by 7–9 radial rows of distorted, small tracheids with thick cell walls. Compared to tracheids formed before the injuring event took place, subsequent growth was abruptly re-established with the formation of tracheids that generally were larger but with distinctly thinner walls. The amount of parenchyma is significantly higher after the event ring, whereas parenchyma cells are somewhat larger and more irregularly shaped (Text-fig. 6a).

In the central part of the event ring, nearly 40 % of the stem wood is overgrown by thin-walled poorly organised cells forming callus parenchyma (Text-fig. 5c).

The latter has overgrown superficially desiccated wood, which is indicated by wedge-shaped cracks extending radially centripetally from the injury (Text-fig. 5b). The surface of the exposed wood is smooth, but shows minor deformation of the secondary xylem and a distinct, 25 mm wide furrow in the middle of the injured zone (Text-fig. 5b). Secondary xylem grew from both margins towards the centre of the injured zone, where it closed the wound completely by anastomosis of tissue (Text-fig. 5d). The growth direction is recognisable by curved tracheid rows and tree rings tapering towards and ceasing at the wounded area.

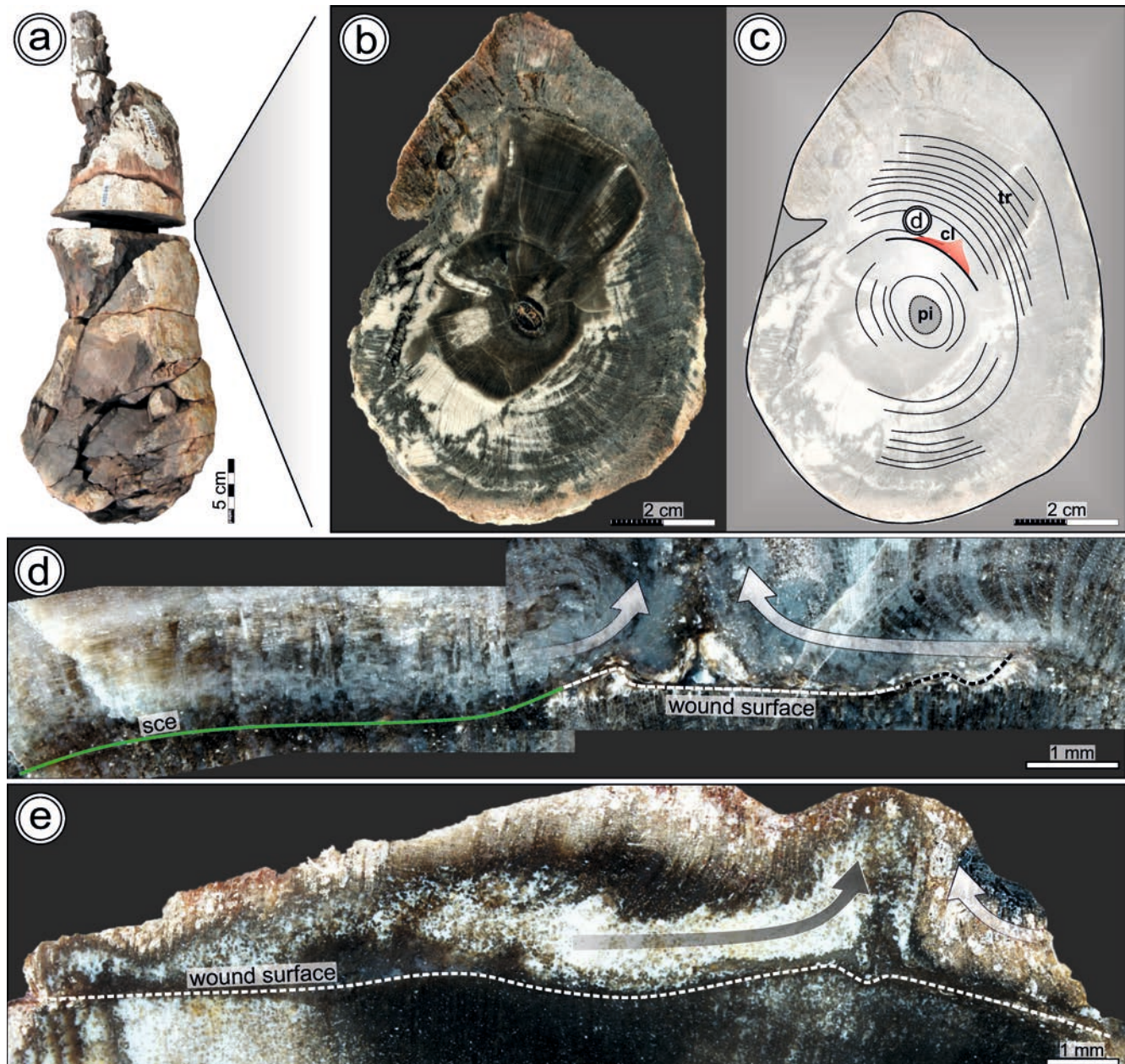
The same injury zone also occurs in sections E, F and H, with nearly the same width. In contrast to section G, in section E the injury zone shows an uneven surface, probably caused by mechanical deformation of the secondary xylem, as well as a much thinner portion of callus (Text-fig. 7a–c). In section C, the injured

Text-fig. 7. Scar morphology in middle to upper sections E and C. **a** – Transverse section E, poorly preserved and representing only a part of the whole stem. **b** – Sketch based on image of “a”, showing part the scar (pi – suggested pith, cl – callus tissue, sce – scar-associated event ring, rc – radial desiccation crack, tr – tree rings; letter shows position of the following image). **c** – Panorama image showing parts of the scar morphology with an irregular wound surface and multiple overgrowths by callus tissue from left to right (arrows). **d** – Polished section C, which shows fragmentary preservation and poorly preserved outer wood. **e** – Sketch based on image of “d” showing the poorly preserved outer wood (light yellow colour), the small scar in “f” and an extraxylary layer, which has been removed on one side of stem by the entombing pyroclastic density current (pi – suggested pith, cl – callus tissue, tr – tree rings, el – extraxylary layer; letter shows position of the following image). **f** – Morphology of the partial scar showing oriented overgrowth of callus tissue (arrow) and scar-associated band/event ring (green colour).



zone diminishes (Text-fig. 7d–f), suggesting a distinct narrowing from the base upwards to a height of ca. 1 m above ground level. In sections A, B and D, the injury zone is not visible, due to a poor cellular preservation in the corresponding stem areas (Text-fig. 4).

Besides the major injury zone, two additional small injuries causing callus growth reaction are observed in the innermost wood of section G, preceding the major wounding event (Text-fig. 5f, g).



Text-fig. 8. Scar morphology in two roots (KH0546 and KH0554) attached to the stem of KH0277. **a** – Anatomically reconstructed first order root KH0546 (modified from RÖßLER et al. 2014). **b** – Transverse section in original growth orientation (modified from RÖßLER et al. 2014). **c** – Sketch based on transverse section showing position of the scar and tree rings (pi – suggested pith, cl – callus tissue, tr – tree rings; number shows position of the following image). **d** – Microscopic panorama image of the root scar in KH0546 with wounded surface overgrown by callus tissue (arrows) and scar-associated event ring (sce, green colour). **e** – Scar in the outermost wood of a small root (KH0554) with overgrown callus tissue (arrows).

4.3 Root damage

Specimen KH0546 represents a partially well-preserved first order root of the *Astromyelon* type, which was found still attached to the basal KH0277 stem (RÖBLER et al. 2014). The root dips sub-horizontally in a NE direction, 50–100 mm below the ground surface into the palaeosol (Text-figs 4, 8a). In a transverse section of 98 × 69 mm diameter in medial position from the stem, a distinct scar is clearly visible in the inner part of the wood, oriented upwards (Text-fig. 8b, c). The scar is only 4 mm wide and asymmetrically overgrown by callus tissue (Text-fig. 8d). Morphologically, minor damage is visible at the secondary xylem. Similar to the scar in section G of KH0277-04, a short band of distorted tracheids is associated with the scar (Text-fig. 8d). The root transverse section shows poorly preserved regular tree rings, indicating that at least ten rings have formed after the injuring event (Text-fig. 8c).

Another scar with overgrown callus tissue was found in the outer wood of a small root, KH0554. The second first order root KH0545 shows no scar in transverse section (Text-fig. 8e).

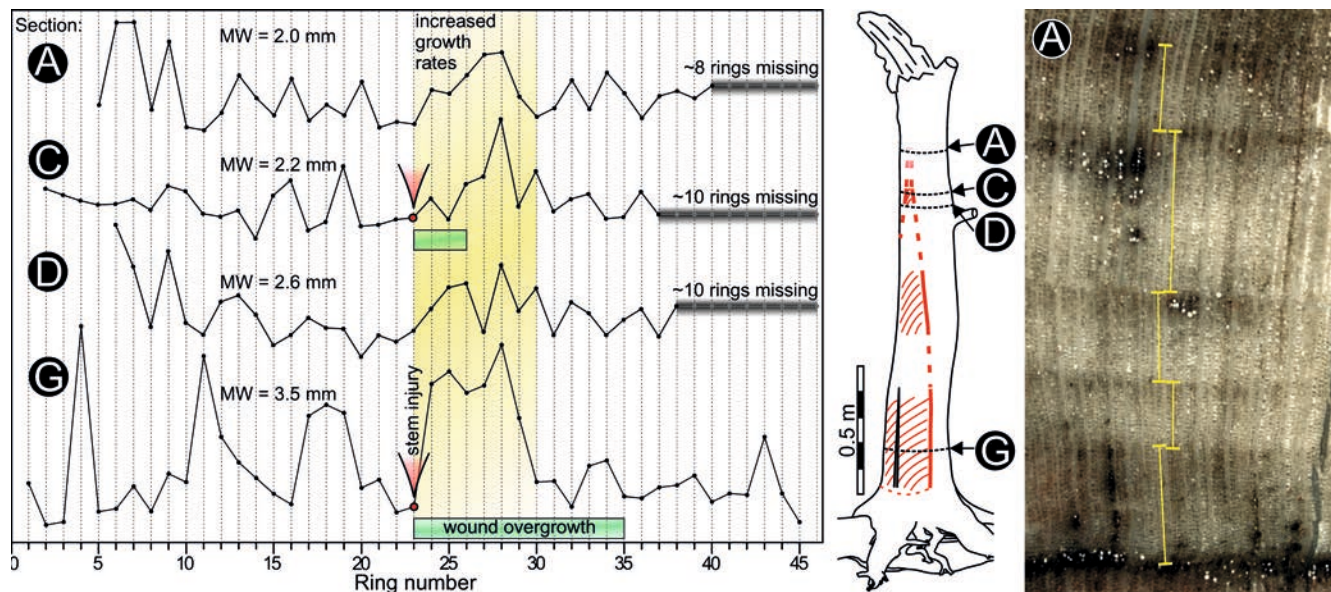
4.4 Tree-ring record

Tree rings were counted in sections A, C, D and G (Text-fig. 9). Although correlation of ring sequences

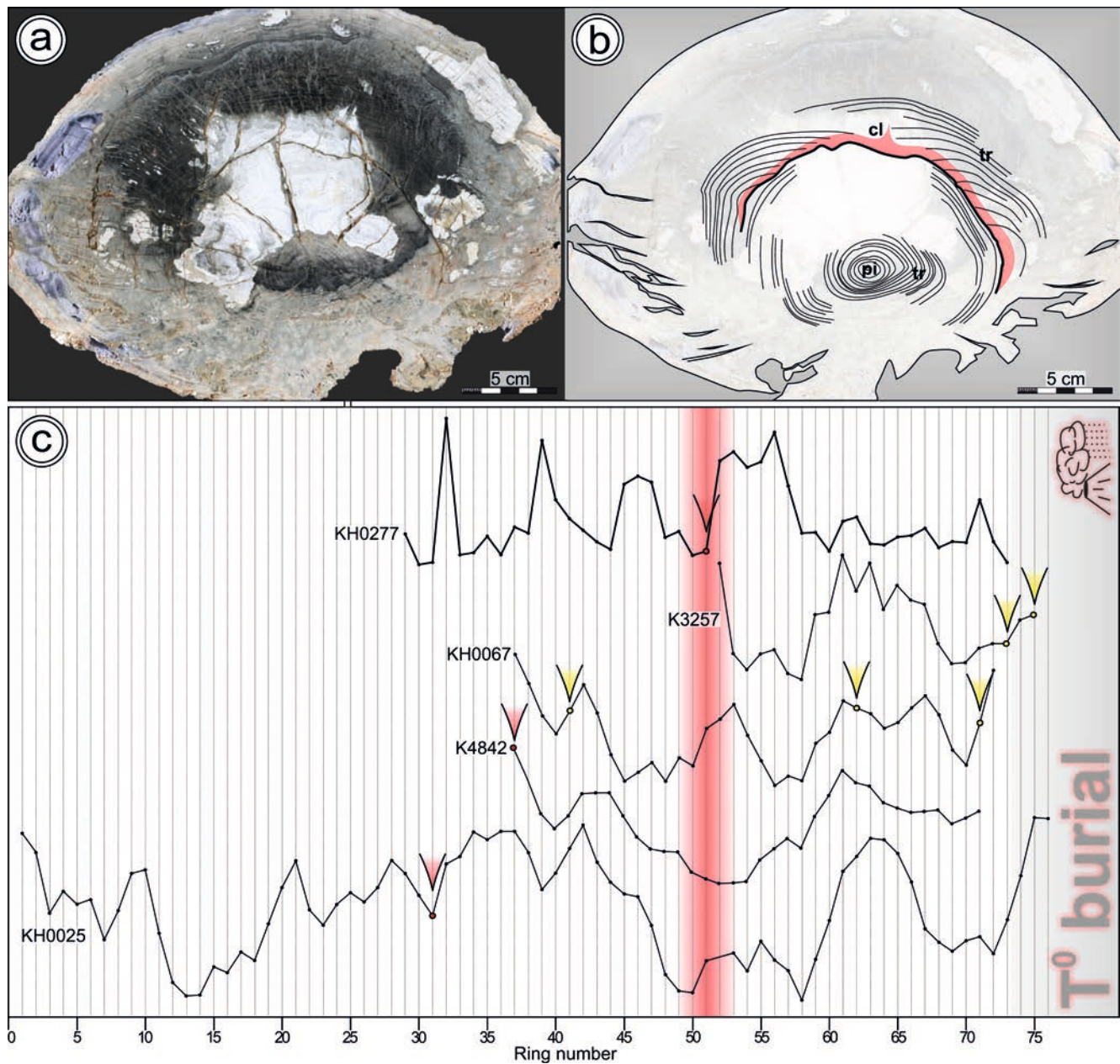
is not statistically proven, their patterns show several similarities as expected since the sections have been cut within a distance of 1.15 m in the same stem. In sections A, C and D, 42–44 tree rings were counted, including 8–10 of the outermost rings, which were excluded from ring width measurements because of inadequate preservation. Forty-five tree rings were counted in section G, over 1 m below section D. The mean ring width (MW) of all measured sections is 2.63 mm; mean sensitivity is 0.43. From base to top, ring width in the sections generally decreases (Text-fig. 9). In section G, the scar occurs after the 22nd ring; after the 35th ring the wound is completely overgrown by newly formed tissue. In section C, the small scar occurs after the 21st ring, thus suggesting that this scar is an elongation of the large scar in section G. All sections show that annual growth before the injuring event was comparatively low. After the event, wide tree rings formed in all of the measured sections, showing that annual growth increased significantly for several years, before reducing again to normal growth rates.

4.5 Periphery of KH0277

In the periphery of KH0277, the palaeosol, in which the tree was rooted, as well as neighbouring trees and branches on the forest ground, were examined for evidence that would clarify the circumstances that caused the injury to the tree.



Text-fig. 9. Tree-ring record of sections A, C, D and G, and their position in the KH0277 basal stem: graphs in diagrams show variations of ring width in measured ring sequences (image); ring width data was detrended and power-transformed; sections A, C and D have distorted tree rings in their outer wood, which were only counted and not measured.



Text-fig. 10. Record of event rings and scars in trees at the same locality, which lived at the same time as KH0277. **a** – Polished transverse section of a horizontally embedded cordaitalean trunk (KH0025) from the Chemnitz-Hilbersdorf excavation site. **b** – Sketch based on transverse section from “a” showing position of a large scar in the inner wood (pi – pith, cl – callus tissue, tr – tree rings). **c** – Diagram of selected ring width curves from the Hilbersdorf locality (K3257, K4842) and the Chemnitz-Hilbersdorf excavation (KH0277, KH0067, KH0025) showing Type 3b/c event rings (yellow tags) and scars of Type 3a event rings (red tags) showing the singularity of the injuring event in KH0277 (red shaded line). Correlation of ring curves is not statistically validated, but partly approximated from similar curve shapes and partly on the more or less simultaneous growth stop after the T^0 volcanic event.

4.5.1 The palaeosol – former substrate of the *in situ* tree

A detailed description of the palaeosol profile is provided by LUTHARDT et al. (2016). The upper 0.40 m are characterised as a sandy, well-drained, but imma-

ture palaeosol of the alluvial floodplain (Text-fig. 1e). It is densely rooted by different types and sizes of roots. Sedimentological indications on potential hazardous depositional or erosional events during the growth of

vegetation, such as rock avalanche or debris flow deposits, are absent. Remains of charcoal as potential evidence for palaeo-wildfire were not found. Within a radius of ca. 5 m in a northern direction from KH0277, an accumulation of deadwood fragments of various sizes was found, mainly embedded in the upper palaeosol horizon (e.g., RÖBLER et al. 2012b: 820, fig. 4D). The majority of these pieces have been preliminarily identified as cordaitalean wood, such as the flattened trunk on which KH0277 was rooted (RÖBLER et al. 2014).

4.5.2 Crown remains

In the near vicinity of KH0277, many adpressions of calamitalean branches and leafy twigs were found in Unit S5.1, a low-energy ash fall deposit. Thus, these finds were most likely part of the foliage of KH0277. A calamitalean branch (KH0293/KH0294) was found embedded in Units S4 and S5, ca. 2.5 m south of KH0277. According to RÖBLER et al. (2012b), the specimen is described as an upside-down entombed stem portion of a calamitalean, which contains silicified body segments of a diplopod and associated coprolites indicating that wood decay had begun. As no significant horizontal transportation is assumed for this branch, it seems likely that it also originated from the KH0277 crown.

4.5.3 Neighbouring trees of KH0277

Besides several smaller stems of calamitaleans, medullosan seed ferns and psaroniacean tree ferns, specimens KH0008 and KH0018 represent large upright cordaitalean trees once growing within a radial distance of ca. 4.5 m of KH0277 (Text-fig. 2a–c). Based on their basal diameters, an original height of ca. 29 m can be estimated for KH0008 and ca. 24 m for KH0018 using the approximation of MOSBRUGGER et al. (1994), which is in accordance to estimated heights of cordaitalean trees from dryland habitats (FALCON-LANG & BASHFORTH 2004; BASHFORTH et al. 2014). Another calamitalean tree, KH0042, grew within a distance of 5.7 m of KH0277, pointing to an estimated original height of ca. 17 m according to MOSBRUGGER et al. (1994) and ca. 20 m according to NIKLAS (1994). Altogether, these three trees are the only *in situ* specimens in the excavation area, which are thought to have been of similar age or older than KH0277. However, none of the associated trees seems to show any indications of a major injury comparable to that seen in KH0277. In this context, it must be

noted that wood anatomical features are hardly recognisable due to inadequate preservation.

In contrast, the horizontally embedded cordaitalean trunk (KH0025) found in Unit S3 shows a distinct injury extending to 40 % of the stem circumference, similar to the injury in KH0277. However, in the tree-ring record of KH0025, 44 rings were counted from the injuring event to the outer margin, whereas in KH0277 only 22 rings are present, suggesting two hazardous events within a time span of ca. 20 years (Text-fig. 10a, b).

From the 53 transverse sections from the Chemnitz-Hilbersdorf site, investigated in LUTHARDT et al. (2017), 33 specimens have a record of more than 22 tree rings. From these 33 specimens, only five exhibit Type 3 event rings. However, as these event rings seem to show a more or less wide chronological spreading, none of these event rings could be clearly correlated with the injury in KH0277 (Text-fig. 10c).

5 Discussion

In the T⁰ assemblage of the Chemnitz Fossil Forest interactions among organisms and their environment are challenging to investigate and interpret, but are highly important for understanding the palaeoecology of the fossil biota. Analysis of the origin of the scar in KH0277 gives an idea of how to approach these multifaceted relationships and how they could be deciphered.

5.1 Reconstruction of KH0277

Calamitaleans are a diverse group of self-supporting, semi-self-supporting and liana-like plants, which represented a major constituent in late Paleozoic forest ecosystems (e.g., FREYTET et al. 2002; PFEFFERKORN et al. 2008; GALTIER 2008; GALTIER et al. 1997; GALTIER et al. 2011; DIMICHELE & FALCON-LANG 2012; MENCL et al. 2013; FALCON-LANG 2015; NEREGATO et al. 2015; NEREGATO et al. 2017). In the early Permian, many anatomically preserved plants from fossil localities of both the Northern and Southern hemispheres suggest a preference for alluvial plain environments characterised by mineral soils and seasonal droughts (RÖBLER 2006; WANG et al. 2006; CAPRETZ & ROHN 2013; RÖBLER et al. 2014; TAVARES et al. 2014; LUTHARDT et al. 2016). From Chemnitz, some of the largest and most complete specimens are known, showing a quite high diversity (RÖBLER & NOLL 2006; RÖBLER & NOLL 2010). In

the Chemnitz-Hilbersdorf excavation, calamitaleans of the genus *Arthropitys* (GOEPPERT 1864) have been reconstructed as more than 15 m high, free-standing trees with highly branched, extensive secondary root systems (RÖBLER et al. 2014), and considerable branching towards the top forming a three-dimensional slender crown (RÖBLER et al. 2012a; FENG et al. 2012). A similar growth architecture can be assumed for KH0277. The stem of KH0277 shows at least three large side shoots recognised already in the basal stem section, which are supposedly only few years old, based on tree rings (Text-fig. 3e, f). The secondary xylem of the *Arthropitys* specimens, including KH0277, shows a particularly high parenchyma portion of ca. 45 % (Text-fig. 3c), which is suggested to have had a water storage function as an adaptation to seasonal droughts (e.g., RÖBLER & NOLL 2006; RÖBLER et al. 2012a; NEREGATO et al. 2015). Based on tree height estimations, the cordaitaleans KH0008 and KH0018 were overtopping the calamitaleans KH0277 and KH0042 by several metres. Thus, it can be assumed that calamitaleans constituted the second storey at the Chemnitz-Hilbersdorf site. Similar relative tree heights were reconstructed for calamitaleans in Pennsylvanian swamp forests (TAYLOR et al. 2009).

Calamitaleans of Pennsylvanian lowland environments are supposed to have had a thin extraxylary layer (BÉTHOUX et al. 2004; DIMICHELE & FALCON-LANG 2012). In Chemnitz, calamitaleans rarely show such thin cortex tissue, which is probably the result of incomplete preservation (RÖBLER et al. 2012a). The outermost wood of KH0277 was covered by a thin layer of extraxylary cortical tissue, but in contrast to previous finds it shows a characteristic internal structure. The palisade-like arrangement of voids or canals could be compared to similar cortical structures that have already been documented by RENAULT (1893: pl. LVI, fig. 6), depicting one of the rare specimens in which the cortex of a (probably rather juvenile) calamitalean is well-preserved. These structures might be anatomically comparable to air-filled vallicular canals in modern *Equisetum*. The type and function of the extraxylary layer in KH0277 remains unknown, as preservation does not allow for more detailed examinations.

With regard to the contrasting poorly and well-preserved areas in sections A-D of KH0277 (Text-fig. 7e), the question about general vitality of the tree arises. Poorly preserved areas convey the impression that major parts of the wood had already been decomposed before petrification started. Features in the

branch of KH0294 further support advanced wood decomposition in the tree. However, there is no reliable evidence supporting this hypothesis. Numerous adpressions of calamitalean leafy twigs in the vicinity of KH0277, in the lowermost ash layer (Unit S5.1), indicate fresh foliation and thus still active metabolism in the tree before it was buried by pyroclastics.

5.2 Potential causes of damage

To evaluate potential causes of the injury in KH0277, the comparison with modern analogies is necessary, as processes leading to tree damage can be easily observed. Comparable scars and their various causes are well investigated in modern trees, predominantly motivated by economic forest management purposes (e.g., HARTIG 1897; KUČERA et al. 1985). Recently, research mainly focusses on reconstructing the chronology of natural hazards to evaluate past and future trends, as well as to improve risk management (e.g., GRISSINO-MAYER & SWETNAM 2000; STOFFEL & BOLLSCHWEILER 2008). Destructive environmental impact on trees can be mechanically, biologically or climatically induced, whereas damaging effects occur in the crown, cambium and/or the roots (SCHWEINGRUBER 2001). Among the most commonly discussed causes are wildfires, lightning strikes, severe frost and droughts, intense solar radiation, hail events, debris flows, avalanches, rock fall, floods, volcanic activity, falling neighbour trees, arthropod feeding and animal scarring (SCHWEINGRUBER 1996; STOFFEL et al. 2010) (Table 1). An evaluation process was used to falsify the listed causes based on their typical damage patterns, including analysis of potential effects on neighbouring trees and the associated substrate. Important characteristics are penetration depth (wood/stem surface), loss of secondary xylem, position in the stem (basal/elevated/whole stem), the shape of the scar (oval/triangular/elongated/irregular), affected plant organs (stem/branches/leaves/roots), special characteristics such as feeding traces, charcoal remains or sedimentary deposits, but also the impact on the closest neighbourhood (individual tree/group of trees).

Macroscopic features of the scar recognised in KH0277 show major damage to both cortex and cambium in section G. Cortex removal may have resulted in desiccation of the wood, indicated by radial cracks (Text-fig. 5b). Minor damage to the secondary xylem is indicated by a central vertical furrow, an irregular scar surface in section E (Text-fig. 7b, c) and

Table 1. Various types of tree damage, their wood anatomical characteristics and impact on periphery. Data is predominantly derived from studies on modern tree damage in gymnosperms, which are regarded as the best fitting modern analogies for fossil calamitaleans from Chemnitz.

Damage type	Tree damage characteristics	Effects on periphery	Literature (selection)
Wildfire	(Wood)/cambium/bark damage, crown/stem/root potentially affected, triangular to oval shaped scars, basal stem position, usually no loss of secondary xylem, initial growth suppression after fire, ring separation, basal sprouting	Neighbouring trees usually affected, charcoal remains	ARBELLAY et al. (2014); BAKER & DUGAN (2013); BROWN & SWETNAM (1994); BYERS et al. (2014); GUTSELL & JOHNSON (1996); SMITH & SUTHERLAND (2001)
Lightning stroke	(Wood)/cambium/bark damage, crown/stem/root potentially affected, elongated and narrow scar, frequently along the whole stem, spiral or straight, central furrow, probably loss of secondary xylem	Rarely death of several neighbouring trees (Blitzloch)	HARTIG (1897); TAYLOR (1965); KUČERA et al. (1985)
Severe frost	Cambium damage in frost rings, wood damage in elongated, short-distant radial cracks	Several trees in the whole ecosystem affected	SCHWEINGRUBER (2001); SCHWEINGRUBER et al. (2006)
Severe drought	Cambium damage in drought rings, wood damage in radial desiccation cracks	Several trees in the whole ecosystem affected	BARNETT (1976)
Intense solar insolation	Bark/cambium damage, multiple callus overgrowth	Several neighbouring trees may be affected	(personal observations)
Hail event	Bark/cambium damage, elongated scars, usually on upper surface of twigs (or stems), partial leaf and crown damage	Several trees may be affected	SCHWEINGRUBER (2001)
Flood/debris flow/ avalanches/ pyroclastic flow	(Wood)/cambium/bark damage, no loss of secondary xylem but gouging, scar oval shaped, slightly above the stem basis, growth suppression/release after event, ring separation	Majority of neighbouring trees affected, sediment deposition/erosion, toppled trees	STOFFEL & BOLLSCHWEILER (2008); STOFFEL & HITZ (2008); STOFFEL et al. (2010); SCHNEUWLY ET AL. (2009); BALLESTEROS et al. (2010); STOFFEL & KLINKMÜLLER (2013)
Rock fall/neighbouring tree	Wood/cambium/bark damage, tangential scratch or impact marks (gouged secondary xylem)	Rarely neighbouring trees	
Arthropod frass	Wood/cambium/bark damage, usually small scars of variable shape and position, feeding traces, fecal pellets	Several trees (of same species) may be affected	FALCON-LANG et al. (2015), FENG et al. (2015; 2017)
Animal scarring	Wood/cambium/bark damage, in crown/stem/roots, predominantly in basal stem, abrupt growth reduction or cessation, scratch marks	Several trees may be affected	SCHWENKE (1978), SCHWEINGRUBER (1996)

gouged tracheid rows in section G (Text-fig. 5d). The more or less triangular shape of the scar is shown in the three-dimensional reconstruction (Text-fig. 4). Due to the fact that only the basal stem is preserved, nearly no data on potential effects on the crown and upper stem parts is available. Nevertheless, identified deadwood pieces lying on or slightly below the former forest ground in the periphery of KH0277 suggests that no major calamitalean branches may have accumulated during the last decades before the volcanic eruption started entombment of the forest. Microscopic features from the associated zone of distorted tracheids in section G shows that the destructive event suddenly occurred, probably at the end of the growing season, which is indicated by prior latewood formation (Text-fig. 6). Correlation of the KH0277-04 (section G) ring sequence among other ring sequences from trees of the same habitat shows that there is no chronologically equivalent event ring (Text-fig. 10c). Thus, the damaging event probably is restricted to the individual of KH0277.

With regard to the palaeogeographic position in the palaeotropics at 10–15° N (BLAKEY 2008), avalanches and severe frost events are unlikely. Severe droughts, intense solar insolation and hail events are realistic scenarios regarding palaeoclimatic reconstructions and are, in the case of severe droughts, responsible for minor event ring formation in calamitaleans and medullosan seed ferns (LUTHARDT et al. 2016; LUTHARDT et al. 2017), but usually do not cause large scars in basal stem parts of trees. As the forest ecosystem was thriving on an alluvial plain predominantly built up of low-energy sedimentary deposits (SCHNEIDER et al. 2012), debris flow and rock fall events can also be excluded. In contrast, flood events could have played a certain role in forest ecosystem dynamics, which may be indicated by large deadwood fragments embedded in the upper sediment of the palaeosol (RÖBLER et al. 2012b). However, this must have been occurred before KH0277 started growing, as it is rooting on such a deadwood fragment. Although the forest was growing in a volcanically active environment, we can exclude damage by pyroclastics, because the stem was injured on the opposite side of the eruption centre, from which the ecosystem was buried, ca. 20 years later (Text-fig. 10c). Though recognised in several trees within the Chemnitz Fossil Lagerstätte, there is no direct evidence for arthropod frass or animal scarring in KH0277, as there are no boring or feeding traces, fecal pellets, major loss of secondary xylem or scratch marks.

As a result, wildfire and a lightning strike are regarded as the most likely scenarios causing the injury in KH0277. In its general habit, the injured zone with an associated event ring of distorted tracheids resembles what was described as a fire scar in Triassic fossil wood from Arizona (Chinle Formation, BYERS et al. 2014). The more or less triangular shape of the scar in KH0277 and its basal position could provide another indication for fire damage (BAKER & DUGAN 2013). However, charcoal remains are lacking in the palaeosol. Additionally, a palaeo-wildfire, even though spatially restricted, should have affected at least some of the neighbouring trees in this densely vegetated environment. Among *in situ* neighbouring trees, and also among many other arborescent plants of the Chemnitz-Hilbersdorf site, no indications of palaeo-wildfire have been observed. The isolation of the damaging event in the forest stand thus points to a lightning strike. Lightning strikes several thousands of trees worldwide every day, whereas the extent of damage ranges from no obvious injury to almost complete destruction of the tree (TAYLOR 1969). Frequently, a characteristic vertical crack or furrow is observed in affected modern trees (HARTIG 1897; TAYLOR 1965), similar to those recorded in sections F–H of KH0277. Lightning scars are usually elongated and extend more or less straight or spiral along the stem, whereas cambium damage increases towards the stem base (HARTIG 1897). These observations from modern trees seem to be in dissent to the scar shape of KH0277, which shares similarity to the shape of a fire scar. In several cases, however, lightning causes ignition or local fire (TAYLOR 1969). With a direct impact, lightning discharge leads to major cambium damage and distortion of the outer living cells of the wood, which is clearly indicated by the scar associated event ring of distorted cells in KH0277 (Text-fig. 3b, e). Cell distortion is supposed to result from rapid water loss or steam pressure by heat development, disturbance of the electrolytic equilibrium and/or temporary collapse of water conductivity (KUČERA et al. 1985). Bark flaking is another common feature resulting from lightning strikes, leading to wood exposition and initiating callus overgrowth, as it is documented in section G of KH0277 (Text-fig. 3b, d). Moreover, contrary to usual fire scars, a lightning strike frequently extends to damage the roots, as discharge proceeds from the stem via the roots into the soil (KUČERA et al. 1985). The distinct scars in two of the first order roots of KH0277 (Text-fig. 8) would further support the lightning hypothesis. A problem arises with regard to tree heights,

because the neighbouring cordaitaleans KH0008 and KH0018 were several metres higher and thus more prone to lightning strikes than KH0277. However, the statistical chance of lightning strikes is not purely dependent on tree height, as smaller trees in a forest stand also exhibit lightning scars (HARTIG 1897). The water, oil and starch content of a tree also are important factors (KUČERA et al. 1985). The amount of living tissue and associated water storage capacity are much higher in parenchyma-rich calamitaleans (Text-fig. 3c) compared to the gymnospermous homoxyls (e.g., RÖBLER & NOLL 2006; RÖBLER et al. 2012a; NEREGATO et al. 2015). Therefore, calamitalean wood rich in electrically conductive soft tissue could make them more lightning prone than other trees, such as the neighbouring taller cordaitaleans.

In conclusion, we suggest that KH0277 could have been injured by a lightning strike, which probably caused restricted ignition at its stem base. Nevertheless, scars resulting from different causes can generally share similarities. Hence, we cannot completely exclude alternative interpretations, such as flood, abrasion by a falling neighbour tree or local wildfire, although these causes seem to be less likely.

Injuries of variable shapes and sizes were found in several additional transverse sections from the Chemnitz-Hilbersdorf excavation and among collected material of the Chemnitz Fossil Lagerstätte, providing some insight into the diversity of growth disturbances in the forest. For example the existence of a large scar in the KH0025 cordaitalean trunk demonstrates the recurrence of severe tree-damaging events within a spatially restricted environment (Text-fig. 10). Once recognised, these fossilised relicts of hazardous events in woody plants potentially provide insight into intricate plant-environment interactions and plant survival strategies in fossil forest ecosystems.

5.3 Plant recovery response

Severe injuring events can lead to various consequences for trees vitality, ranging from sudden death to complete recovery. In most cases, wounds are potential weak spots, as they produce exposed stem areas, which can be easily colonised by pathogenic and parasitic (micro-)organisms (e.g. SHIGO 1984). Thus, damaging environmental forces act as important controls on tree vitality in a forest ecosystem (FRANCIS et al. 1987). In turn, vitality and adaptation strategies are important factors determining to which degree a tree recovers from growth disturbances. In response

to an injury, abrupt growth changes such as formation of a barrier zone, poorly organised parenchyma cells, bulge-like overgrowth of callus tissue and production of resin ducts and secretory channels are among the most common plant responses (SCHWEINGRUBER 2001).

In KH0277, the impact on living tissue was severe, as ca. 40 % of the cambium and ca. 75 % of the outermost active xylem were damaged in the basal stem. Nevertheless, morphological characteristics of the scar suggest a rapid and almost complete recovery. Based on the tree-ring record, a healing time of ca. 12 years was estimated in section G (Text-fig. 9), which appears to be a remarkably small time span in comparison with modern analogies. BAKER & DUGAN (2013) reported on healing processes of fire scars in *Pinus ponderosa* in Northern Arizona (USA), estimating a mean healing time of 38 years, but up to 80 years in large scars. Initial formation of small and crumpled tracheids suggests that the injuring event caused a period of hampered secondary growth or even quiescence, which was followed by a phase of rapid secondary growth indicated by large, thin-walled tracheids (Text-fig. 6). In all measured ring sequences, tree rings show a sudden increase in ring width after the injuring event, probably as a whole-tree stress response (Text-fig. 9). Section G shows initial growth of an adventitious shoot in response to the injury, suggesting stress-induced basal sprouting (Text-fig. 3e). Rapid closure of the wound may have prevented the tree from major invasion by fungi or wood-boring insects, as no feeding traces or decomposed wood areas are visible in direct contact to the scar.

6. Conclusions

1. Injuries in fossil trees result from various causes, but remain poorly investigated. We suspect that such injuries occur more frequently than has thus far being documented. Investigation of tree injuries has the potential to shed light on multifaceted plant-environment interactions in ancient forested landscapes.
2. The T⁰ character of the Chemnitz Fossil Lagerstätte allows for the investigation of specific plant-environment interactions in an early Permian, volcanically preserved forest ecosystem, both in space and time.
3. The calamitalean KH0277 represents the basal stem of an *Arthropityx bistrinata* tree found in growth position. The tree is reconstructed as a

free-standing individual ca. 20 m high, and probably constituted to the second storey in the forest architecture, several metres below the tallest cordaitaleans.

4. Basal stem sections of KH0277 and two of its first order roots show distinct scars in the secondary xylem, which resulted from a sudden, severe environmental impact, whereas neighbouring trees apparently were unaffected. The most plausible scenario for the formation of the injury is a lightning strike, which probably caused ignition or locally restricted fire at the stem base.
5. The calamitalean completely recovered from its severe injury within a comparably short time period of 12 years. Rapid growth rates in the whole basal stem and basal sprouting are regarded as stress-induced plant physiological reactions in response to the damage.

Acknowledgements

We highly acknowledge the technical and scientific support by VOLKER ANNACKER (Chemnitz) and ROBERT NOLL (Tiefenthal). We thank TRISTAN ROSCHER (Deutschneudorf) and HUBERT BIESER for technical support in preparation works. We are deeply grateful for the kind contribution by SIDNEY R. ASH (Albuquerque, New Mexico), BRUCE BYERS (Falls Church, Virginia), HENRI GRISSINO-MEYER (Knoxville, Tennessee) and MARKUS STOFFEL (Zurich), for sharing their expertise and for fruitful discussion. We want to highlight the financial support by the Deutsche Forschungsgemeinschaft within a 3-year-research project (DFG grant RO 1273/3-1 to RR). The manuscript considerably benefited from the review of ARDEN ROY BASHFORTH (Copenhagen) and the editorial work of LUTZ KUNZMANN (Dresden).

References

- ARBELLAY, E., STOFFE, M., SUTHERLAND, E. K., SMITH, K. T. & FALK, D. A. (2014): Changes in tracheid and ray traits in fire scars of North American conifers and their ecophysiological implications. – *Ann. Bot.*, **114**: 223–232.
- BAKER, W. A. & DUGAN, A. J. (2013): Fire-history implications of fire scarring. – *Can. J. Forestry Res.*, **43**: 951–962.
- BALLESTEROS, J. A., STOFFEL, M., BODOQUE, J. M., BOLL-SCHWEILER, M., HITZ, O. & DÍEZ-HERRERO, A. (2010): Changes in Wood Anatomy in Tree Rings of *Pinus pinaster* Ait. Following Wounding by Flash Floods. – *Tree-Ring Res.*, **66** (2): 93–103.
- BARNETT, J. R. (1976): Rings of collapsed cells in *Pinus radiata* stemwood from lysimeter-grown trees subjected to drought. – *New Zeal. J. Forest Sci.*, **6** (2): 461–465.
- BASHFORTH, A. R., CLEAL, C. J., GIBLING, M. R., FALCON-LANG, H. J. & MILLER, R. F. (2014): Paleocology of Early Pennsylvanian vegetation on a seasonally dry tropical landscape (Tynemouth Creek Formation, New Brunswick, Canada). – *Rev. Palaeobot. Palynol.*, **200**: 229–263.
- BÉTHOUX, O., GALTIER, J. & NEL, A. (2004): Earliest evidence of insect endophytic oviposition. – *Palaios*, **19**: 408–413.
- BLAKEY, R. C. (2008): Gondwana paleogeography from assembly to breakup – a 500 million year odyssey. – In: FIELDING, C. R., FRANK, T. D. & ISBELL, J. L. (eds): *Resolving the Late Paleozoic Ice Age in Time and Space*. – *Geol. Soc. Am. Spec. Pap.*, **441**: 1–28.
- BROWN, P. M. & SWETNAM, T. W. (1994): A cross-dated fire history from coast redwood near Redwood National Park, California. – *Can. J. Forestry Res.*, **24**: 21–31.
- BYERS, B. A., ASH, S. R., CHANEY, D. & DESOTO, L. (2014): First known fire scar on a fossil tree trunk provides evidence of Late Triassic wildfire. – *Palaeogeogr. Palaeoclimatol. Palaeoecol.*, **411**: 180–187.
- CAPRETZ, R. L. & ROHN, R. (2013): Lower Permian stems as fluvial paleocurrent indicators of the Parnaíba Basin, northern Brazil. – *J. South Am. Earth Sci.*, **45**: 69–82.
- DI MICHELE, W. A. & FALCON-LANG, H. J. (2011): Fossil forests in growth position (T^0 assemblages): origin, taphonomic biases and palaeoecological significance. – *J. Geol. Soc. London*, **168** (2): 585–605.
- DI MICHELE, W. A. & FALCON-LANG, H. J. (2012): Calamitalean “pith casts” reconsidered. – *Rev. Palaeobot. Palynol.*, **173**: 1–14.
- DUNLOP, J. A. & RÖBLER, R. (2013): The youngest trigonotarbid from the Permian of Chemnitz in Germany. – *Foss. Rec.*, **16** (2): 229–243.
- DUNLOP, J. A., LEGG, D. A., SELDEN, P. A., FET, V., SCHNEIDER, J. W. & RÖBLER, R. (2016): Permian scorpions from the Petrified Forest of Chemnitz, Germany. – *BMC Evol. Biol.*, **16** (1): 72.
- EULENBERGER, S., TUNGER, B. & FISCHER, F. (1995): Neue Erkenntnisse zur Geologie des Zeisigwaldes bei Chemnitz. – *Veröff. Mus. Naturkunde Chemnitz*, **18**: 25–34.
- FALCON-LANG, H. J. (2015): A calamitalean forest preserved in growth position in the Pennsylvanian coal measures of South Wales: Implications for palaeoecology, ontogeny and taphonomy. – *Rev. Palaeobot. Palynol.*, **214**: 51–67.
- FALCON-LANG, H. J. & BASHFORTH, A. R. (2004): Pennsylvanian uplands were forested by giant cordaitalean trees. – *Geology*, **32** (5): 417–420.
- FALCON-LANG, H. J., LABANDEIRA, C. C. & KIRK, R. (2015): Herbivorous and detritivorous arthropod trace-fossils associated with sub-humid vegetation in the Middle Pennsylvanian of southern Britain. – *Palaios*, **30**: 192–206.
- FENG, Z., ZIEROLD, T. & RÖBLER, R. (2012): When horsetails became giants. – *Chinese Sci. Bull.*, **57** (18): 2285–2288.
- FENG, Z., RÖBLER, R., ANNACKER, V. & YANG, J.-Y. (2014): Micro-CT investigations of a seed fern (probable medullosan) fertile pinna from the Early Permian Petrified Forest in Chemnitz, Germany. – *Gondwana Res.*, **26**: 1208–1215.

- FENG, Z., SCHNEIDER, J.W., LABANDEIRA, C.C., KRETZSCHMAR, R. & RÖBLER, R. (2015): A specialized feeding habit of Early Permian oribated mites. – *Palaeogeogr. Palaeoclimatol. Palaeoecol.*, **417**: 121–125.
- FENG, Z., WANG, J., RÖBLER, R., ŚLIPINŃSKI, A. & LABANDEIRA, C.C. (2017): Late Permian wood-borings reveal an intricate network of ecological relationships. – *Nature Communications*, **556** (8): 1–6.
- FISCHER, F. (1990): Lithologie und Genese des Zeisigwald-Tuffs (Rotliegendes, Vorerzgebirgs-Senke). – *Veröff. Mus. Naturkunde Chemnitz*, **14**: 61–74.
- FRANCIS, J. F., SHUGART, H. H. & HARMON, M. E. (1987): Tree death as an ecological process – The causes, consequences, and variability of tree mortality. – *BioScience*, **37** (8): 550–556.
- FREYDET, P., GALTIER, J., RONCHI, A., SCHNEIDER, J. W., TINTORI, A. & WERNEBURG, R. (2002): Early Permian continental biota from Southeastern Sardinia (Ogliastra and Gerrei). – *Rend. Soc. Paleont. Ital.*, **1**: 169–176.
- GALTIER, J. (2008): A new look at the permineralized flora of Grand-Croix (Late Pennsylvanian, Saint-Etienne basin, France). – *Rev. Palaeobot. Palynol.*, **151**: 129–140.
- GALTIER, J., DAVIERO, V. & MEYER-BERTHAUD, B. (1997): Découverte de fragments de troncs d'arbres perminéralisés dans le bassin Stéphanien de Graissessac (Sud du Massif Central, France). – *Geobios*, **20**: 243–247.
- GALTIER, J., RONCHI, A. & BROUTIN, J. (2011): Early Permian silicified floras from the Perdasdefogu Basin (SE Sardinia): comparison and bio-chronostratigraphic correlation with the floras of the Autun Basin (Massif central, France). – *Geodiversitas*, **33** (1): 43–69.
- GASTALDO, R. A., PFEFFERKORN, H. W. & DIMICHELE, W. A. (1995): Characteristics and classification of Carboniferous roof shale floras. – *Geol. Soc. Am., Memoirs*, **185**: 341–352.
- GOEPPERT, H. R. (1864): Die fossile Flora der Permischen Formation. – *Palaeontographica*, **12**: 1–124.
- GOEPPERT, H. R. (1881): Pathologie und Morphologie fossiler Stämme. – *Palaeontographica*, **28**: 1–12.
- GRISSINO-MAYER, H. D. & SWETNAM, T. W. (2000): Century-scale climate forcing of fire regimes in the American Southwest. – *Holocene*, **10**: 213–220.
- GUTSELL, S. L. & JOHNSON, E. A. (1996): How fire scars are formed: coupling a disturbance process to its ecological effect. – *Can. J. Forestry Res.*, **26**: 166–174.
- HARTIG, R. (1897): Untersuchung über Blitzschläge in Waldbäumen. – *Forstlich-naturwissenschaftliche Zeitschrift*, **6** (3): 97–120.
- KUČERA, L. J., EICHENBERGER, B. & STOLL, A. (1985): The lightning gap – cause and development. – In: KUČERA, L. J. (ed.): *Xylorama – Trends in wood research*. – pp. 127–138 (Springer) Basel.
- LUTHARDT, L. & RÖBLER, R. (2017a): Fossil forest reveals sunspot activity in the early Permian. – *Geology*, **45** (3): 279–282.
- LUTHARDT, L. & RÖBLER, R. (2017b): Jahresringe in den Bäumen des Versteinerten Waldes von Chemnitz und die aus ihnen ableitbaren paläoklimatologischen und paläoökologischen Erkenntnisse. – *Veröff. Mus. Naturkunde Chemnitz*, **40**: 43–68.
- LUTHARDT, L., RÖBLER, R. & SCHNEIDER, J. W. (2016): Palaeoclimatic and site-specific conditions in the early Permian fossil forest of Chemnitz – sedimentological, geochemical and palaeobotanical evidence. – *Palaeogeogr. Palaeoclimatol. Palaeoecol.*, **441**: 627–652.
- LUTHARDT, L., RÖBLER, R. & SCHNEIDER, J. W. (2017): Tree-ring analysis elucidating palaeo-environmental effects captured in an in situ fossil forest – The last 80 years within an early Permian ecosystem. – *Palaeogeogr. Palaeoclimatol. Palaeoecol.*, **487**: 278–295.
- LUTHARDT, L., HOFMANN, M., LINNEMANN, U., GERDES, A., MARKO, L. & RÖBLER, R. (2018): A new U–Pb zircon age and a volcanogenic model for the early Permian Chemnitz Fossil Forest. – *Int. J. Earth Sci.* doi: 10.1007/s00531-018-1608-8
- MENCL, V., HOLEČEK, J., RÖBLER, R. & SAKALA, J. (2013): First anatomical description of silicified calamitalean stems from the upper Carboniferous of the Bohemian Massif (Nová Paka and Rakovník areas, Czech Republic). – *Rev. Palaeobot. Palynol.*, **197**: 70–77.
- MOSBRUGGER, V., GEE, C. T., BELZ, G. & ASHRAF, A. R. (1994): Three-dimensional reconstruction of an in-situ Miocene peat forest from the Lower Rhine Embayment, northwestern Germany – new methods in palaeovegetation analysis. – *Palaeogeogr. Palaeoclimatol. Palaeoecol.*, **110**: 295–317.
- NEREGATO, R., RÖBLER, R., ROHN, R. & NOLL, R. (2015): New petrified calamitaleans from the Permian of the Parnaíba Basin, central-north Brazil. Part I. – *Rev. Palaeobot. Palynol.*, **215**: 23–45.
- NEREGATO, R., RÖBLER, R., IANNUZZI, R., NOLL, R. & ROHN, R. (2017): New petrified calamitaleans from the Permian of the Parnaíba Basin, central-north Brazil, part II, and phytogeographic implications for late Paleozoic floras. – *Rev. Palaeobot. Palynol.*, **237**: 37–61.
- NIKLAS, K. J. (1994): The allometry of safety-factors for plant height. – *Am. J. Bot.*, **81** (3): 345–351.
- PFEFFERKORN, H. W., GASTALDO, R. A., DIMICHELE, W. A. & PHILLIPS, T. L. (2008): Pennsylvanian tropical floras from the United States as a record of changing climate. – In: FIELDING, C. R., FRANK, T. D. & ISBELL, J. L. (eds): *Resolving the Late Paleozoic Ice Age in Time and Space*. – *Geol. Soc. Am. Spec. Pap.*, **441**: 305–316.
- RENAULT, B. (1893): Bassin houiller et permien d'Autun et d'Épinac, flore fossile, 2e partie. – In: *Études des gîtes minéraux de la France, IV. Atlas*. – (Imprimerie Nationale) Paris.
- RÖBLER, R. (2000): The late Palaeozoic tree fern *Psaronius* – an ecosystem unto itself. – *Rev. Palaeobot. Palynol.*, **108** (1): 55–74.
- RÖBLER, R. (2006): Two remarkable Permian Petrified Forests: correlation, comparison and significance. – *Geol. Soc. London Spec. Publ.*, **265**: 39–63.

- RÖßLER, R. & NOLL, R. (2006): The largest known anatomically preserved calamite, an exceptional find from the Petrified Forest of Chemnitz, Germany. – *Rev. Palaeobot. Palynol.*, **140**: 145–162.
- RÖßLER, R. & NOLL, R. (2010): Anatomy and branching of *Arthropitys bistriata* (COTTA) GOEPPERT. New observations from the Permian Petrified Forest of Chemnitz, Germany. – *Int. J. Coal Geol.*, **83**: 103–124.
- RÖßLER, R., ANNACKER, V., KRETZSCHMAR, R., EULENBERGER, S. & TUNGER, B. (2008): Auf Schatzsuche in Chemnitz – Wissenschaftliche Grabungen '08. – *Veröff. Mus. Naturkunde Chemnitz*, **31**: 5–44.
- RÖßLER, R., KRETZSCHMAR, R., ANNACKER, V. & MEHLHORN, S. (2009): Auf Schatzsuche in Chemnitz – Wissenschaftliche Grabungen '09. – *Veröff. Mus. Naturkunde Chemnitz*, **32**: 25–46.
- RÖßLER, R., KRETZSCHMAR, R., ANNACKER, V., MEHLHORN, S., MERBITZ, M., SCHNEIDER, J. W. & LUTHARDT, L. (2010): Auf Schatzsuche in Chemnitz – Wissenschaftliche Grabungen '10. – *Veröff. Mus. Naturkunde Chemnitz*, **33**: 27–50.
- RÖßLER, R., FENG, Z. & NOLL, R. (2012a): The largest calamite and its growth architecture – *Arthropitys bistriata* from the Permian petrified forest of Chemnitz. – *Rev. Palaeobot. Palynol.*, **185**: 64–78.
- RÖßLER, R., ZIEROLD, T., FENG, Z., KRETZSCHMAR, R., MERBITZ, M., ANNACKER, V. & SCHNEIDER, J. W. (2012b): A snapshot of an Early Permian ecosystem preserved by explosive volcanism: new results from the petrified forest of Chemnitz, Germany. – *Palaeo*, **27**: 814–834.
- RÖßLER, R., MERBITZ, M., ANNACKER, V., LUTHARDT, L., NOLL, R., NEREGATO, R. & ROHN, R. (2014): The root systems of Permian arborescent sphenopsids: evidence from the Northern and Southern hemispheres. – *Palaeontographica Abt. B*, **291** (4–6): 65–107.
- SCHNEIDER, J. W., LUCAS, S. G., WERNEBURG, R. & RÖßLER, R. (2010): Euramerican Late Pennsylvanian/Early Permian arthropleurid/tetrapod associations – implications for the habitat and paleobiology of the largest terrestrial arthropod. – *New Mexico Museum of Natural History and Sci. Bull.*, **49**: 49–70.
- SCHNEIDER, J. W., RÖßLER, R. & FISCHER, F. (2012): Rotliegend des Chemnitz-Beckens. – In: Deutsche Stratigraphische Kommission: Stratigraphie von Deutschland X. Rotliegend. Teil I: Innervariatische Becken. – *Schriftenreihe Dt. Ges. Geowiss.*, **61**: 530–588.
- SCHNEUWLY, D. M., STOFFEL, M. & BOLLSCHWEILER, M. (2009): Formation and spread of callus tissue and tangential rows of resin ducts in *Larix decidua* and *Picea abies* following rockfall impacts. – *Tree Phys.*, **29**: 281–289.
- SCHWEINGRUBER, F. H. (1996): *Tree Rings and Environment Dendroecology*. – pp. 1–609 (Paul Haupt) Bern.
- SCHWEINGRUBER, F. H. (2001): *Dendroökologische Holzanatomie: Anatomische Grundlagen der Dendrochronologie*. – pp. 1–472 (Paul Haupt) Bern.
- SCHWEINGRUBER, F. H., BÖRNER, A. & SCHULZE, E.-D. (2006): *Atlas of Woody Plant Stems: Evolution, Structure, and Environmental Modifications*. – pp. 1–229 (Springer) Berlin.
- SCHWENKE, W. (1978): *Die Forstschädlinge Europas*. Vol. 3. – pp. 1–467 (Parey) Hamburg.
- SHIGO, A. L. (1984): Compartmentalization: A conceptual framework for understanding how trees grow and defend themselves. – *Ann. Rev. Phytopathol.*, **22**: 189–214.
- SMITH, K. T. & SUTHERLAND, E. K. (2001): Terminology and biology of fire scars in selected central hardwoods. – *Tree-Ring Res.*, **57** (2): 141–147.
- SPINDLER, F., WERNEBURG, R., SCHNEIDER, J. W., LUTHARDT, L., ANNACKER, V. & RÖßLER, R. (2018): First arboreal 'pelycosaurs' (Synapsida: Varanopidae) from the early Permian Chemnitz Fossil Lagerstätte, SE-Germany, with a review of varanopid phylogeny. – *Pal. Z.*, **92** (1): 315–364. doi: 10.1007/s12542-018-0405-9
- STOFFEL, M. & BOLLSCHWEILER, M. (2008): Tree-ring analysis in natural hazards research – an overview. – *Nat. Hazards Earth Syst. Sci.*, **8**: 187–202.
- STOFFEL, M. & HITZ, O. M. (2008): Rockfall and snow avalanche impacts leave different anatomical signatures in tree rings of juvenile *Larix decidua*. – *Tree Phys.*, **28**: 1713–1720.
- STOFFEL, M. & KLINKMÜLLER, M. (2013): 3D analysis of anatomical reactions in conifers after mechanical wounding: first qualitative insights from X-ray computed tomography. – *Trees*, **27** (6): 1805–1811.
- STOFFEL, M., BOLLSCHWEILER, M., BUTLER, D. R. & LUCKMAN, B. H. (2010): Tree rings and natural hazards. – In: BENISTON, M. (ed.): *Advances of Global Change Research*, **41**: 1–486.
- TAVARES, T. M. V., RÖßLER, R., NOLL, R. & ROHN, R. (2014): Petrified Marattiales pinnae from the Lower Permian of North-Western Gondwana (Parnaíba Basin, Brazil). – *Rev. Palaeobot. Palynol.*, **201**: 12–28.
- TAYLOR, A. R. (1965): Diameter of lightning as indicated by tree scars. – *J. Geophys. Res.*, **70** (22): 5693–5695.
- TAYLOR, A. R. (1969): Tree-bole ignition in superimposed lightning scars. – *USDA Forest Serv. Res. Note INT-90*: pp. 1–4.
- TAYLOR, T. N., TAYLOR, E. L. & KRINGS, M. (2009): *Paleobotany – The Biology and Evolution of Fossil Plants*. 2nd ed. – pp. 1–1230 (Elsevier and Academic Press) Amsterdam.
- WANG, S. J., HILTON, J., GALTIER, J. & TIAN, B. (2006): A large anatomically preserved calamitean stem from the Upper Permian of southwest China and its implications for calamitean development and functional anatomy. – *Pl. Syst. Evol.*, **261**: 229–244.